Journal of Molecular Neuroscience (2022) 72:336–348
https://doi.org/10.1007/s12031-021-01936-1

Paeonol Ameliorates Cognitive Deficits in Streptozotocin Murine Model of Sporadic Alzheimer's Disease via Attenuation of Oxidative Stress, Inflammation, and Mitochondrial Dysfunction

Akram Tayanloo-Beik[1] · Zahra Kiasalari[2] · Mehrdad Roghani[2]

Received: 16 September 2021 / Accepted: 20 October 2021 / Published online: 19 November 2021

Abstract

Intracerebroventricular (ICV) microinjection of diabetogenic drug streptozotocin (STZ) in rodents consistently produces a model of sporadic Alzheimer's disease (sAD) which is characterized by tau pathology and concomitant cognitive decline, insulin resistance, neuroinflammation, oxidative stress, and mitochondrial malfunction. Paeonol is an active phenolic component in some medicinal plants like Cortex Moutan with neuroprotective efficacy via exerting anti-inflammatory and anti-oxidative effects. This study was conducted to assess beneficial effect of paeonol in amelioration of cognitive deficits in ICV STZ rat model of sAD. STZ (3 mg/kg) was microinjected into the lateral ventricles on days 0 and 2, and paeonol was given p.o. at two doses of 25 (low) or 100 (high) mg/kg from day 0 (post-surgery) till day 24 post-STZ. Cognitive performance was evaluated in different tasks, and oxidative stress- and inflammation-related parameters were measured in addition to immunohistochemical assessment of glial fibrillary acidic protein (GFAP) as a marker of astrocytes. Paeonol at the higher dose ameliorated cognitive deficits in Barnes maze, novel object recognition (NOR) task, Y maze, and passive avoidance test. In addition, paeonol partially reversed hippocampal malondialdehyde (MDA), reactive oxygen species (ROS), total antioxidant capacity (TAC), superoxide dismutase (SOD), catalase, glutathione reductase, tumor necrosis factor α (TNFα), interleukin 6 (IL-6), mitochondrial membrane potential (MMP), myeloperoxidase (MPO), and acetylcholinesterase (AChE) activity. Paeonol treatment was also associated with lower hippocampal immunoreactivity for GFAP. This study showed that paeonol can alleviate cognitive disturbances in ICV STZ rat model of sAD via ameliorating neuroinflammation, oxidative stress, mitochondrial dysfunction, and also through its attenuation of astrogliosis.

Keywords Sporadic Alzheimer's disease · Streptozotocin · Paeonol · Mitochondrial dysfunction · Oxidative stress · Neuroinflammation

Abbreviations

AChE	Acetylcholinesterase
ADS	Alzheimer's disease
GFAP	Glial fibrillary acidic protein
GSH	Glutathione (reduced form)
ICV	Intracerebroventricular
IL-6	Interleukin 6
MDA	Malondialdehyde
MMP	Mitochondrial membrane potential
MPO	Myeloperoxidase
NF-κB	Nuclear factor kappa-light-chain-enhancer of activated B cells
NOD	Novel object discrimination
ROS	Reactive oxygen species
sAD	Sporadic Alzheimer's disease
SOD	Superoxide dismutase
STZ	Streptozotocin
TAC	Total antioxidant capacity
TNFα	Tumor necrosis factor α

✉ Zahra Kiasalari
kiasalari@shahed.ac.ir

✉ Mehrdad Roghani
mroghani@shahed.ac.ir

[1] Department of Biology, School of Basic Sciences, Shahed University, Tehran, Iran

[2] Neurophysiology Research Center, Shahed University, Tehran, Iran

Introduction

Nearly 80% of dementia cases are related to Alzheimer's disease (AD) (Crous-Bou et al. 2017). According to the report of Alzheimer's Association, the number of patients

with AD is expected to rise from about 56 million in 2020 to approximately 88 million in 2050 (Alzheimer's Association 2020). AD causes not only a substantial social impact, but would also lead to a great economic burden imposed on healthcare systems (Oba et al. 2021). Available treatments for AD neither can stop nor delay the progression of the disease process and only provide symptomatic relief (Folch et al. 2016; Mohamad Nasir et al. 2018). The majority of AD patients have late-onset disease, the so-called sporadic AD (sAD) (Masters et al. 2015). Intracerebroventricular (ICV) injection of the diabetogenic drug streptozotocin (STZ) is associated with prominent cognitive impairments in rats (Akhtar et al. 2021; Baluchnejadmojarad and Roghani 2006) and is put forward as a valid model of sAD (Verma et al. 2020). In this model, oxidative stress, neuroinflammation, mitochondrial dysfunction, apoptosis, and cholinergic dysfunction play a substantial role in the development of cognitive decline and neurodegeneration (Rani et al. 2021; Verma et al. 2020; Zameer et al. 2019). Since AD is presented as a multifactorial disorder typified by the existence of amyloid plaques, neurofibrillary tangles, and culminant neuronal death, the search for multitarget and more effective treatments for this prevalent disorder still continues (Martins et al. 2020).

There exists an urgent requirement to develop more effective therapies for treatment and delaying the onset of neurological disorders. Several bioactive compounds isolated from natural products can play a crucial role in the prevention and cure of neurodegenerative disorders including AD (Zhu et al. 2019). Paeonol (20-hydroxy-40-methoxyacetophenone) as a bioactive agent is found in some medicinal plants such as *Paeonia suffruticosa* with numerous advantageous and positive effects, probably due to its anti-inflammatory and free radical scavenging potential (Guo et al. 2020; Kong et al. 2020). Interestingly, paeonol has shown its beneficial and neuroprotective effect in models of neurological disorders including Parkinson's disease (Shi et al. 2016; Ye et al. 2017) and D-galactose and aluminum-induced AD (Han et al. 2020). Additionally, paeonol can lower hippocampal neurotoxicity (Jin et al. 2020) and is effective to mitigate subacute brain injury following cerebral ischemia (Zhao et al. 2018). Beneficial effect of paeonol in ameliorating cognition dysfunction in STZ-induced model of diabetes, partly through decreasing AChE activity and Aβ deposition in the hippocampal tissue, has already been reported (Liu et al. 2013). In addition, neuroprotective potential of paeonol in STZ murine model of diabetes has also been demonstrated, as shown by its prevention of neuronal damage and neuroinflammation (Adki and Kulkarni 2021). Since the effect of paeonol in ICV STZ model of AD has not been reported before, the present study was designed and conducted to explore the possible beneficial effect of this phenolic agent in our model of Alzheimer's like dementia.

Materials and Methods

Subjects

In the current study, a total of 60 male albino Wistar rats weighing 200–250 g were purchased from animal facility of Shahid Beheshti University of Medical Sciences. They were housed 3–4/cage with free access to the food and water under a stable condition for temperature (21–23 °C), light/dark cycle (12 h), and humidity (40–50%). Present study was approved by Institutional Ethics Committee of the Shahed University (Approval ID: IR.SHAHED.REC.1399.042).

Experimental Procedure

Animals were randomly divided into and assigned to five testing groups, each containing 12 rats including the following: 1 — the sham group undergoing sham operation and receiving bilateral intracerebroventricular (ICV) injection of aCSF as the vehicle of STZ and also vehicle of the paeonol (*p.o.*), 2 — Sham + Paeonol 100 which received bilateral ICV injection of aCSF and treated with the paeonol at a dose of 100 mg/kg, 3 — ICV STZ group with bilateral injection of STZ (and also the vehicle of the paeonol, and 4 — STZ + Paeonol 25 which received bilateral ICV injection of STZ and also the paeonol at a dose of 25 mg/kg, and STZ + Paeonol 100 group which received bilateral ICV injection of STZ and also the paeonol at a dose of 100 mg/kg. Composition of aCSF solution consisted of (in mM) 125 NaCl, 3 KCl, 1.15 CaCl2, 0.8 MgCl2, 27 NaHCO3, and 0.33 NaH2PO4 (pH adjusted to 7.4). Paeonol (SigmaAldrich, USA) was dissolved in 10% Cremophor (from SigmaAldrich, USA) and administered up to day 24 after first STZ (Santa Cruz Biotechnology, Inc., USA) microinjection, started 2 h after first ICV STZ injection (day 0). STZ was freshly dissolved in aCSF and bilaterally injected with a Hamilton syringe at a dose of 3 mg/kg and at a volume of 5 µl, two times with an interval of 48 h, i.e., days 0 and 2 (Sharma and Garabadu 2020). Timeline of the study and used protocols have been brought in Fig. 1.

Surgical Procedure

In order to induce the model of sAD in rats, they were first anesthetized using an *i.p.* injection of a mixture of ketamine (100 mg/kg) and xylazine (10 mg/kg). Then, rats were placed in a stereotaxic apparatus (Stoelting Co., USA) where they received ICV injection of STZ (Santa Cruz Biotechnology, Inc., USA) twice at an interval of 48 h. In accordance to Paxinos and Watson stereotaxic atlas (7th edition, 2013), targeting of the lateral ventricles for ICV injection (5 µl/

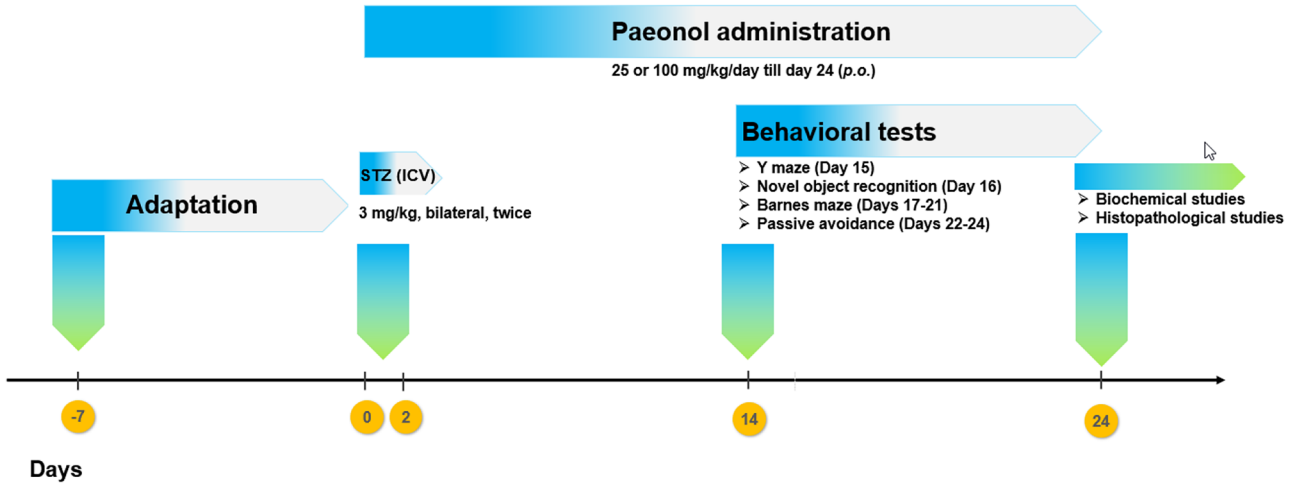

Fig. 1 Experimental and chronological design of the study. Streptozotocin (STZ) was injected *i.c.v.* at a dose of 3 mg/kg twice on days 0 and 2 to induce sporadic model of Alzheimer's disease (sAD). Paeonol was daily given *p.o.* at doses of 25 or 100 mg/kg, started 2 h after first STZ injection till day 24 post-surgery. At weeks 3 and 4 post-surgery, behavioral tests were performed to assess different aspects of cognition

side) was conducted at the following coordinates: −0.8 mm posterior to bregma, 4 mm below dura, and ± 1.4 mm lateral to bregma. ICV microinjection was done using a Hamilton microsyringe. Following the first STZ injection, treatment with paeonol was initiated 2 h after first STZ injection in a daily manner using a gavage needle till day 24 post-surgery. At the start of week 3 post-surgery, behavioral tests were performed for 10 days with a distinct sequence including Y maze, novel object recognition (NOR) test, Barnes maze, and shuttle box (passive avoidance) test. It is worthy to note that treatments were continually applied until the end of the experiments before euthanasia of the animals.

Y Maze Task

For assessing the spatial and recognitive memory, Y maze task was performed according to a previous report (Nasri et al. 2012). Three labeled and equal-sized arms were arranged at an angle of 120° relative to each other, and rats were freely allowed to start passing through them for 8 min, and their entrance order was monitored and noted. Overlapping in the entrance to the different triple arms was assumed as true alternation. Finally, total number of entrances-2 was regarded as the maximum possible alternations and the ratio of actual to possible alternations was calculated as the alternation.

Novel Object Discrimination (Recognition) Task

The recognition ability of the rats was evaluated in novel object task according to earlier studies (Stuart et al. 2013). Following the adaptation, each rat underwent two exploration trials, each 5 min, with an interval of 4 h. Totally, this test included two sessions. In session 1 (familiarization session), exploration of two similar objects was done by the rats. Exploration behavior of the rats was noted considering points including sniffing, licking, or moving the vibrissae toward the object. In session 2 (retention and recall phase), one of the objects was replaced by a new (novel) object with different shape, size, and color and rats were allowed to explore the objects. The calculation of the discrimination ratio (index) was performed as follows: $(t[\text{novel}] - t[\text{familiar}])/(t[\text{novel}] + t[\text{familiar}]) \times 100$.

Passive Avoidance Paradigm

After adaptation, this test was done in two sessions, as reported before (Ahshin-Majd et al. 2016). The acquisition session and retention and recall session are two major steps in this test. In the first session, the rat was placed in the light chamber and after 10 min, the lamp was turned on, and guillotine interconnecting door was raised. Here, the initial latency was assumed as the time needed for entering the dark chamber. Then, an electric shock (1 mA, 1 ms) was applied with the aim of providing a conditioned behavior. In the retention and recall session, time spent by the rat for passing through the light chamber and entering the dark chamber was served as step-through latency (STL) with a cut-off time of 180 s.

Spatial Memory Assessment in Barnes Maze

This maze was employed to judge precisely spatial aspects of memory processes according to previous investigations

(Zappa Villar et al. 2018, 2020). In short, the maze consisted of an elevated circular platform, 120 cm in diameter, containing 20 circular holes around its periphery, each 10 cm in diameter and positioned radially. The escape hole was designated as hole 0, while the other holes were numbered as 1 to 10 clockwise, and as −1 to −9 counterclockwise. A white-light 500-W lamp provided the required aversive stimulus to force animals to discover the escape box. The escape box under hole 0 was filled with appropriate bedding material. At the beginning of the test, rats were adapted to the task. At acquisition sessions, the animals were placed in the starting chamber, situated at the central area of the platform for 1 min, and then, the chamber was elevated and the aversive stimuli (light) was switched on and the animals were allowed to explore the maze for 2 min. Probe trial session was analogous to acquisition trials except that the escape box was removed. Behavioral parameters obtained from this maze were as follows: latency as the time a rat spent since its release from the starting box until it enters the escape box during acquisition trial or the first exploration of escape box during probe trial and errors as the number of explorations of holes aside from the escape box. Each exploration of an incorrect hole was regarded as an error, on condition that the rat lowered its nose below the plane of the surface. The maze was cleaned with 70% alcohol before testing rats individually.

Tissue Homogenate Preparation

On 24th day after first ICV injection of STZ, all rats were anesthetized with ketamine (150 mg/kg), perfused (transcardial procedure) with cold heparinised normal saline, and decapitated using a rat guillotine and brain tissues were quickly removed. Some brains ($n=5$/group) were transferred to 4% paraformaldehyde fixative solution in 0.1 M phosphate buffer and were used for immunohistochemical assessment and the remaining specimens ($n=6$–7/group) were used for biochemical evaluation. For the latter measurement, both right and left hippocampi were dissected out, weighed, and homogenized in cold Tris–HCl buffer (150 mM, pH 7.4) to make 10% (w/v) homogenate preparation. For instance, if their weights were 0.1 g, we used 1 ml of lysis buffer to make a 10% homogenate and so on. The homogenates were then centrifuged at 7000 × g for 10 min at 4 °C. Finally, the supernatant was aliquoted and frozen at −80 °C for next assays.

Quantity of total protein in the lysate was determined by specific bicinchoninic acid (BCA) kit (Kiazist, Iran) with its protocol reported before (Walker 1996). The principle of this experiment is that proteins can reduce Cu + 2 to Cu + 1 under an alkaline condition which turns purple in the presence of BCA. In this test, 50 µl of sample was added to 50 µl of prepared working reagent and kept at 55 °C for 30 min. After cooling, absorbance was read at 560 nm employing a microplate reader.

Measurement of Hippocampal TNF and Il-6

For this assay, sandwich ELISA protocol was used with specific primary and secondary (HRP-conjugated) antibodies provided from Santa Cruz Biotechnology, Inc., USA. Results were finally reported as pg/mg of protein.

Measurement of Oxidative Stress-Related Parameters

Malondialdehyde (MDA) is reported to be mainly responsible for cytopathological effects seen during oxidative stress of lipid peroxidation (Esterbauer et al. 1991). Estimation of MDA as a reliable marker of lipid peroxidation was performed by thiobarbituric acid (TBA) method as mentioned in earlier studies (Olszewska-Słonina et al. 2011). The supernatants were mixed with a combination of TBA and trichloroacetic acid in HCl to precipitate protein. The reaction was performed under boiling conditions for 30 min. The formed precipitate was isolated through centrifugation at 3000 × *g* at room temperature for 10 min. Absorption of samples was read at a wavelength of 532 nm. Final concentration of MDA was expressed as nmol MDA/mg of protein.

Estimation of ROS level was performed using dichlorofluorescein-diacetate (DCF-DA) probe (Arya et al. 2013; Ramazi et al. 2020). In this test, fluorescence intensity is directly proportional to the ROS level. In this experiment, 10 µlof 10 µM non-fluorescent DCF-DA was added to 100 µl of lysate and incubated for 40 min at 37 °C in dark. Then, fluorescence intensity according to quantity of formed fluorescent DCF was read at 488 nm excitation and 525 nm emission and results were reported as arbitrary fluorescence unit (AFU).

Nitrite level indicating the amount of nitric oxide generation was measured according to Griess reaction which has been reported before (Wopara et al. 2021). In this assay, equal volumes of tissue lysate and Griess reagent (0.1% N-(1-naphthyl) ethylenediamine-dihydrochloride and 1% sulfanilamide in 5% phosphoric acid) were mixed and incubated in dark for 10 min at room temperature. Then, the absorbance of the reaction mixture was read at 540 nm.

Total antioxidant capacity (TAC) of samples was measured as reported before (Benzie and Strain 1996). In this test, 135 µl of freshly prepared FRAP (TAC) reagent consisting of sodium acetate buffer (pH 3.6), 2,4,6-tri(2-pyridil)-s-triazine (TPTZ) and ferric chloride were mixed with 15 µl of tissue homogenate. After incubation at 37 °C for 15 min, absorbance was read at 550 nm, and results were reported as nmol/mg protein.

Level of GSH (reduced form) in tissue lysate was measured using reduced glutathione (GSH) kit (SigmaAldrich, USA) and according to earlier reports (Ojha et al. 2015). In this test, samples were deproteinized with a solution of 5% 5-sulfosalicylic acid, centrifuged to exclude the precipitated protein, and the obtained supernatant was used for measurement of GSH. Ten microliters of supernatant were added to 150 µl of working reagent containing assay buffer, 5,5′-dithiobis (2-nitrobenzoic acid) (DTNB), and GSH reductase for 5 min. Then, 50 µl of diluted NADPH solution was added and mixed. Absorbance was read at 412 nm, and results were brought as nmol/mg protein.

To assess and measure the activity of antioxidant enzymes consisting of superoxide dismutase (SOD) and catalase, specific assay kits from Cayman Chemicals, USA, were employed, as previously reported (Ojha et al. 2015). For catalase, 20 µlof samples and 30 µl of methanol was added to the assay buffer with further addition of 20 µlof hydrogen peroxide. After an incubation for 20 min at room temperature, 30 µl of potassium hydroxide was added with subsequent addition of 30 µl of purpald and 10 µl of potassium periodate. Finally, the absorbance was read at 540 nm. Catalase activity was shown as unit/mg. For superoxide dismutase (SOD) activity, sample and diluted radical detector were added to xanthine oxidase to start the reaction. After an incubation for 30 min at room temperature in a dark room, absorbance was read at 450 nm using a microplate reader. The activity of SOD was shown as Unit/mg.

The activity of glutathione peroxidase was measured according to previous studies (Mohandas et al. 1984; Uddin et al. 2016). The reaction solution consisted of 0.1 M phosphate buffer (pH 7.4), sodium azide, glutathione reductase, GSH, EDTA, NADPH, H2O2, and hippocampal homogenate. Changes of absorbance at 25 °C were determined at 340 nm, and results were reported as nmol/min/mg protein.

For measurement of glutathione reductase, the protocol mentioned in earlier studies was employed (Mohandas et al. 1984; Uddin et al. 2016). The reaction mixture consisted 0.1 M phosphate buffer (pH 7.6), EDTA, NADPH, oxidized glutathione, and tissue homogenate. Changes of absorbance at 25 °C were measured at 340 nm, and results were reported as nmol/min/mg protein.

Measurement of AChE Activity

The method of Ellman was applied to quantify AChE activity (Ellman et al. 1961). In this test, acetyl thiocholine iodide, 5,5-dithio-bis-(2-nitrobenzoic acid) (DTNB), and 50 mM Tris–HCl (pH 8.0) with 0.1% BSA were added and kept at 25 °C for 5 min. Then, absorbance was determined at 405 nm. Thereafter, 25 µl of tissue homogenates was added and absorbance was obtained after incubation for 5 min. The AChE activity was reported as nmol/min/mg protein.

Biochemical Assessment of Mitochondrial Membrane Potential

MMP measurement was done as an overall estimation of mitochondrial function and health, and its protocol has been reported before (Ding et al. 2013; Ma et al. 2010). In this test, sample was centrifuged at 10,000 rpm with the precipitate having mitochondrial fraction. The obtained precipitate was reacted with rhodamine 123 (SigmaAldrich, USA), and MMP was obtained (excitation = 488 nm, emission = 525 nm).

Determination of MPO Activity

Myeloperoxidase (MPO) activity is known as a valid and consistent index of neutrophil infiltration and was measured according to past studies (Khosravi et al. 2019; Pulli et al. 2013). In this test, 10 µl of sample was combined with 80 µl of 0.75 mM H2O2 and 110 µl of tetramethylbenzidine solution and the plate was kept at 37 °C for a period of 5 min. The reaction was stopped by including 50 µl of 2 M H2SO4 (stop solution) and the absorption was read at 450 nm.

GFAP Immunohistochemistry

Paraformaldehyde-fixed hippocampal tissue blocks ($n = 5$/group) were processed and embedded in paraffin. Using a rotary microtome (Leica, Germany), 5-µm-thick coronal sections were prepared and transferred upon glass slides. For immunohistochemistry, sections were reacted using primary antibodies against GFAP (monoclonal, diluted 1:75, Santa Cruz Biotechnology, Inc., USA) followed by their incubation with secondary antibody (HRP-conjugated, 1:75 dilution, Santa Cruz Biotechnology, Inc., USA). Binding was visualized in the presence of 3,3′-diaminobenzidine-tetrahydrochloride (DAB) and counterstained with Hematoxylin for 15 s. To assess and quantify GFAP immunoreactivity (IRA), positive immunoreactive and positive area within the hippocampal stratum radiatum below the CA1 subfield at coronal levels 3.1–3.6 mm posterior to stereotaxic bregma landmark was quantified using the ImageJ software (NIH, Version 1.49) by a trained experimenter who was blind to experimental groups and findings were reported as GFAP-positive areas per mm2.

Statistical Assessment of Data

All presented data are brought as means ± standard error (SE) and were analyzed by statistical software GraphPad Prism 8.4 (GraphPad Software Inc., USA). The data were tested for being normal using Shapiro–Wilk test before proceeding with analysis of variance (ANOVA). In addition, Levene's test was applied to verify homogeneity of

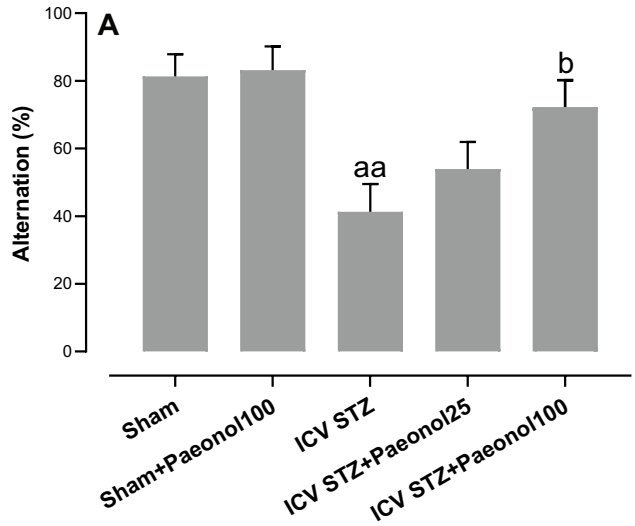
A
Alternation (%)
100
80
60
40
20
0
aa
b
Sham
Sham+Paeonol100
ICV STZ
ICV STZ+Paeonol25
ICV STZ+Paeonol100

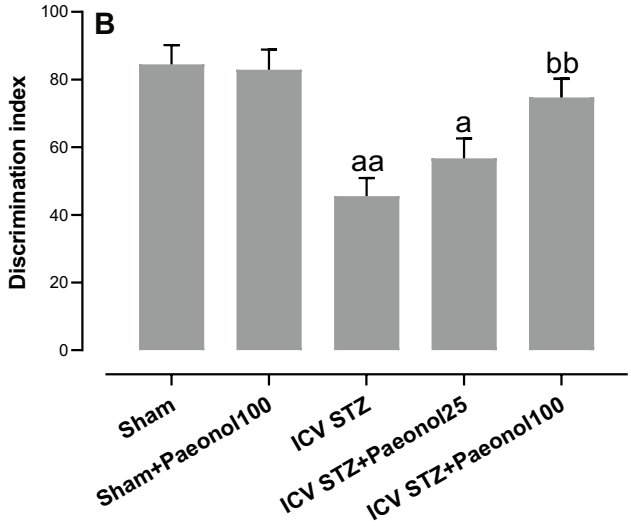
B
Discrimination index
100
80
60
40
20
0
aa
a
bb
Sham
Sham+Paeonol100
ICV STZ
ICV STZ+Paeonol25
ICV STZ+Paeonol100

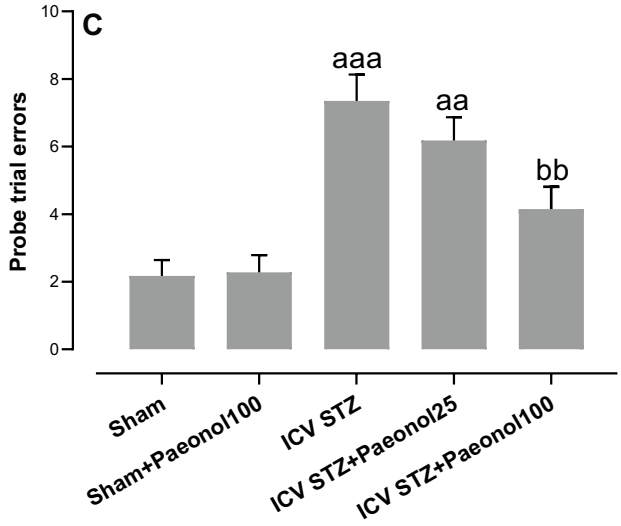
C
Probe trial errors
10
8
6
4
2
0
aaa
aa
bb
Sham
Sham+Paeonol100
ICV STZ
ICV STZ+Paeonol25
ICV STZ+Paeonol100

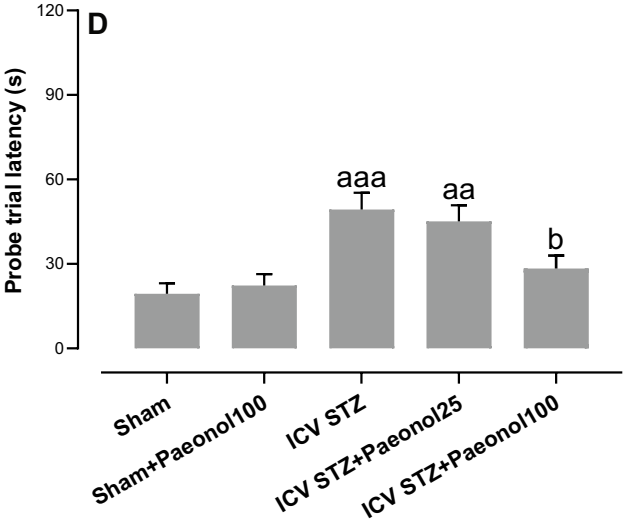
D
Probe trial latency (s)
120
90
60
30
0
aaa
aa
b
Sham
Sham+Paeonol100
ICV STZ
ICV STZ+Paeonol25
ICV STZ+Paeonol100

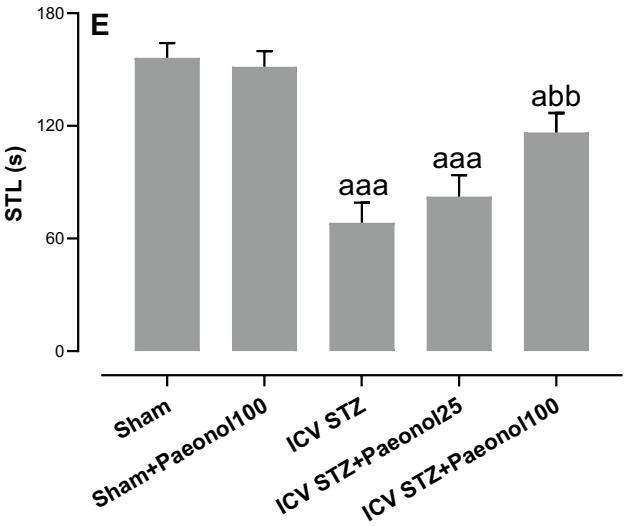
E
STL (s)
180
120
60
0
aaa
aaa
abb
Sham
Sham+Paeonol100
ICV STZ
ICV STZ+Paeonol25
ICV STZ+Paeonol100

◂**Fig. 2** Performance of animals in different cognitive paradigms consisting of Y-maze (**A**), novel object discrimination (NOD) (**B**), Barnes maze (**C**, **D**), and passive avoidance (**E**) tests. Results are brought as means ± SE. $n = 11–12$/group. [a], [aa], and [aaa] indicate $p < 0.05$, $p < 0.01$, and $p < 0.001$, respectively (as compared to the sham group); [b] and [bb] indicate $p < 05$ and $p < 0.01$, respectively (as compared to the ICV STZ group)

variances. Significant differences were found out using one-way analysis of variance with subsequent Tukey's multiple range test, if required. The level of statistical significance shown in results section was based on the p-values $p < 0.05$, $p < 0.01$, and $p < 0.001$.

Results

Behavioral Findings

Behavioral assessment of performance in different tasks including Y-maze (Fig. 2A), novel object discrimination (Fig. 2B), Barnes maze (Fig. 2C–D), and passive avoidance in shuttle box (Fig. 2E) was evaluated in week 3 post-STZ.

Single-session Y maze protocol was used to analyze short-term and spatial recognition memory through assessment of spontaneous unprovoked alternation. Our obtained data (Fig. 2A) showed a significantly lower alternation percentage in rats from ICV STZ group ($p < 0.01$) when compared to relevant data of the control group. In contrast, alternation percentage in ICV STZ group under treatment with paeonol at a dose of 100 mg/kg was significantly greater in comparison with vehicle-treated ICV STZ group ($p < 0.05$) and paeonol the lower dose of 25 mg/kg did not produce such advantageous effect. Meanwhile, no significant effect was observed in the control group receiving paeonol (100 mg/kg) when it was compared with the control group.

Recognitive short-term memory was also judged in novel object recognition (discrimination) task (Fig. 2B). Rats in the ICV STZ group exhibited a significant and prominent fall of discrimination index as compared to the control group ($p < 0.01$). Contrarily, discrimination index was significantly improved in paeonol 100-treated ($p < 0.05$) ICV STZ group and paeonol at a dose of 25 mg/kg did not have such significant effect. In addition, no significant effect of paeonol at a dose of 100 mg/kg was observed in the control group regarding discrimination index.

In order to assess hippocampal-dependent spatial and long-term aspects of memory phenomenon, we conducted Barnes maze task. Our findings showed that there are no statistically significant differences amongst experimental groups regarding errors and latencies as indicators of learning performance in acquisition trials (data not shown). Statistical analysis of memory performance in the probe trial phase showed significantly higher number of errors ($p < 0.001$) and greater latency ($p < 0.001$) in ICV STZ group when compared to the control group (Fig. 2C, D). On the contrary, with paeonol treatment of ICV STZ group at a dose of 100 mg/kg, significantly fewer errors ($p < 0.01$) and less latency ($p < 0.05$) were observed when compared with comparable data of ICV STZ group. In addition, paeonol at a dose of 25 mg/kg did not exert such beneficial effect at a significant level in ICV STZ group. Also, no significant effect was found out for the control group receiving paeonol at a dose of 100 mg/kg in comparison with the control animals for performance in Barnes maze task.

To judge conditioned learning and avoidance memory in mice to find out recall and retention ability, passive avoidance task was employed. Statistical analysis of obtained data showed no significant differences amongst experimental groups regarding transfer latency in the acquisition stage. In contrast, a significant difference was found out in the transfer (step-through) latency time between the experimental groups ($p < 0.01$). Post hoc analysis showed a significant reduction of step-through latency in the ICV STZ group relative to the control group ($p < 0.001$). On the other hand, this latency was properly greater in paeonol 100-treated ICV STZ group versus vehicle-treated ICV STZ group ($p < 0.01$) with no significant effect of paeonol at a dose of 25 mg/kg (Fig. 2E).

Hippocampal Assessment of Oxidative Stress and Inflammation

Hippocampal tissue was evaluated for oxidative stress and inflammation-related parameters in different experimental groups (Table 1). Statistical analysis of obtained data exhibited that hippocampal level of MDA ($p < 0.001$), ROS ($p < 0.001$), nitrite ($p < 0.01$), IL-6 ($p < 0.001$), and TNFα ($p < 0.01$) significantly elevates and level of TAC ($p < 0.01$), GSH ($p < 0.01$), SOD ($p < 0.001$), catalase ($p < 0.01$), glutathione peroxidase ($p < 0.05$), and glutathione reductase ($p < 0.01$) significantly decreases due to ICV STZ challenge and oral administration of paeonol at a dose of 100 mg/kg significantly and properly restored hippocampal levels of MDA ($p < 0.05$), ROS ($p < 0.01$), TAC ($p < 0.05$), SOD ($p < 0.05$), catalase ($p < 0.05$), glutathione reductase ($p < 0.05$), TNFα ($p < 0.01$), and IL-6 ($p < 0.01$) with no significant effect on nitrite, GSH, and glutathione peroxidase as compared with relevant data of vehicle-treated ICV STZ group. Additionally, no significant effect was observed in paeonol-treated ICV STZ group at a dose of 25 mg/kg or for paeonol-treated control group regarding the mentioned parameters.

To assess the effect of ICV STZ on mitochondrial health and integrity, MMP index was measured employing Rhodamine 123 (Table 1). Our findings showed that hippocampal MMP markedly decreases in ICV STZ group ($p < 0.001$) and

Table 1 Hippocampal level of oxidative stress- and inflammation-associated parameters and mitochondrial health

	Sham	Sham + Paeonol 100	ICV STZ	ICV STZ + Paeonol 25	ICV STZ + Paeonol 100
Oxidative stress and antioxidants					
MDA (nmol/mg) *n* = 7/group	1.23 ± 0.11	1.27 ± 0.12	2.15 ± 0.16^{aaa}	1.87 ± 0.15^{a}	1.54 ± 0.15^{b}
Estimated ROS (AFU) *n* = 7/group	2178 ± 229	2073 ± 251	5835 ± 381^{aaa}	5071 ± 395^{aaa}	3541 ± 357^{abb}
Nitrite (µg/mg) *n* = 7/group	7.35 ± 0.68	7.01 ± 0.75	12.32 ± 0.97^{aa}	10.07 ± 0.91	9.15 ± 0.82
TAC (nmol/mg) *n* = 7/group	4.91 ± 0.27	5.07 ± 0.31	2.89 ± 0.35^{aa}	3.17 ± 0.38^{aa}	4.29 ± 0.31^{b}
GSH (nmol/mg) *n* = 7/group	8.35 ± 0.41	8.27 ± 0.43	5.38 ± 0.0.47^{aa}	5.54 ± 0.49^{aa}	6.91 ± 0.47
SOD (unit/mg) *n* = 7/group	7.92 ± 0.35	7.69 ± 0.38	4.91 ± 0.41^{aaa}	5.83 ± 0.35^{aa}	6.42 ± 0.32^{aab}
Catalase (unit/mg) *n* = 7/group	3.09 ± 0.18	2.92 ± 0.16	1.87 ± 0.20^{aa}	1.93 ± 0.18^{aa}	2.63 ± 0.17^{aab}
Glutathione peroxidase (nmol/min/mg) *n* = 7/group	41.36 ± 3.91	40.15 ± 4.03	23.65 ± 4.01^{a}	29.17 ± 3.95	35.49 ± 3.97
Glutathione reductase (nmol/min/mg) *n* = 7/group	83.71 ± 5.85	83.97 ± 6.18	51.72 ± 6.37^{aa}	56.09 ± 6.13^{a}	78.23 ± 6.18^{b}
Inflammation					
TNFα (pg/mg) *n* = 7/group	17.38 ± 1.35	19.35 ± 1.43	36.41 ± 1.95^{aaa}	31.07 ± 1.72^{aaa}	26.34 ± 1.73^{aabb}
IL-6 (pg/mg) *n* = 7/group	15.14 ± 1.19	14.32 ± 1.28	30.83 ± 1.85^{aaa}	26.16 ± 1.88^{aa}	22.35 ± 1.51^{abb}
Mitochondrial membrane potential					
MMP (AFU) *n* = 7/group	100 ± 0.00	97.30 ± 1.38	51.37 ± 5.21^{aaa}	58.31 ± 4.99^{aaa}	78.29 ± 5.05^{aabb}

All data are brought as means ± SEM

AFU arbitrary fluorescence unit, *MDA* malondialdehyde, *ROS* reactive oxygen species, *TAC* total antioxidant capacity, *GSH* reduced glutathione, *SOD* superoxide dismutase, *TNF*α tumor necrosis factorα, *IL-6* interleukin 6, *MMP* mitochondrial membrane potential

$^{a}p < 0.05$

$^{aa}p < 0.01$

$^{aaa}p < 0.001$ (groups statistically compared to the sham group)

$^{b}p < 0.05$

$^{bb}p < 0.01$ (paeonol-treated ICV STZ groups compared to the vehicle-treated ICV STZ group)

paeonol treatment of ICV STZ group at a dose of 100 mg/kg significantly and properly enhanced MMP ($p < 0.01$).

Hippocampal Level of MPO and AChE

Hippocampal activity of MPO as a marker of neutrophil infiltration (Fig. 3A) and AChE activity (Fig. 3B) significantly elevated in ICV STZ group as compared with the sham group ($p < 0.01$). In contrast, paeonol administration to ICV STZ group at a dose of 100 mg/kg properly and significantly attenuated hippocampal activity of both MPO and AChE in relation to vehicle-treated ICV STZ group ($p < 0.05$). In addition, paeonol treatment of ICV STZ group at the lower dose of 25 mg/kg did not produce such beneficial and significant effect.

Immunohistochemical Findings for GFAP

Immunohistochemical assessment of immunoreactivity intensity for GFAP as definite and reliable marker of astrocytes (Kovacs 2017) in the stratum radiatum area of the hippocampus showed that this reactivity is significantly higher in vehicle-treated ICV STZ group when statistically compared to the relevant data of the control group ($p < 0.001$). In contrast, paeonol administration to ICV STZ group at the higher dose of 100 mg/kg significantly lowered reactivity for GFAP ($p < 0.01$) versus ICV STZ group with no significant effect obtained for paeonol at the lower dose of 25 mg/kg. In addition, treatment of the sham group with paeonol at a dose of 100 mg/kg did not produce noticeable and significant changes regarding this parameter (Fig. 4).

Discussion

In the present study, we analyzed behavioral, biochemical, and histopathological changes in the ICV STZ model of sAD and also evaluated the possible efficacy of the bioflavonoid paeonol. Following the administration of paeonol for 24 days to ICV STZ rats at the higher dose of 100 mg/kg, improvement of performance in different behavioral tasks including Y-maze, novel object recognition test, Barnes maze, and passive avoidance test was observed. Additionally, paeonol treatment of ICV STZ groups was dose-dependently associated with lower hippocampal level of oxidative stress and neuroinflammation, attenuation of hippocampal AChE activity, mitochondrial dysfunction, and neutrophil infiltration, and mitigation of astrogliosis.

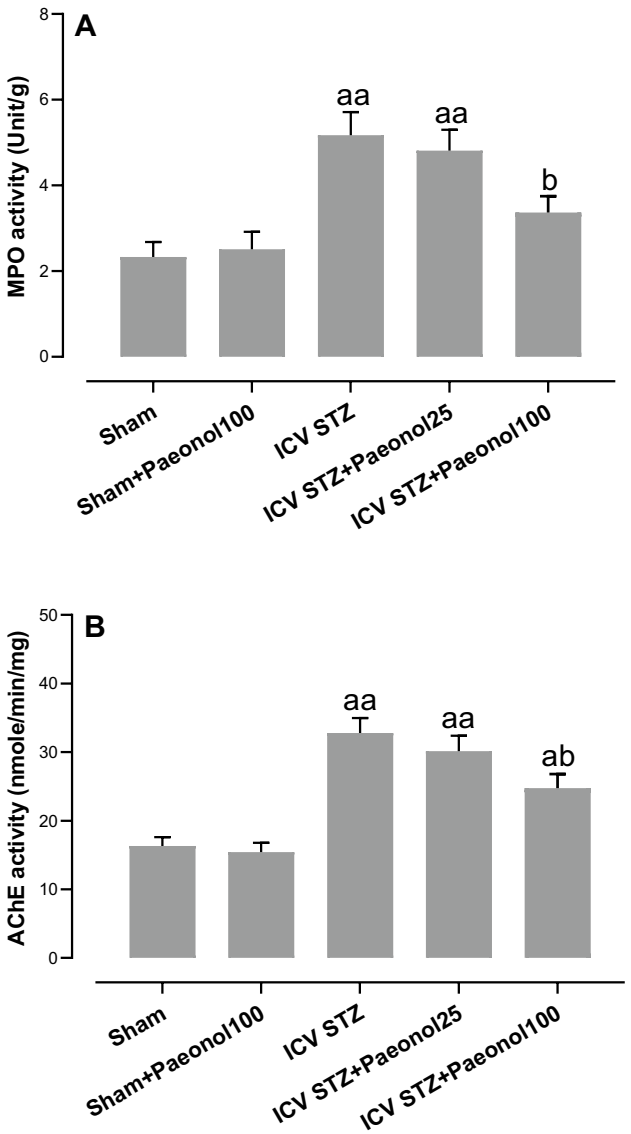

Fig. 3 Hippocampal activity of the enzyme myeloperoxidase as a marker of neutrophil infiltration (**A**) and acetylcholinesterase (AChE) (**B**) in different groups. Results are brought as means ± SE. $n = 7$/group. [a], [aa], and [aaa] indicate $p < 0.05$, $p < 0.01$, and $p < 0.001$, respectively (as compared to the sham group); [b] and [bb] indicate $p < 05$ and $p < 0.01$, respectively (as compared to the ICV STZ group)

Bilateral ICV injection of STZ produces a well-accepted and consistent model to mimic sAD (Verma et al. 2020) with development of cognitive impairments in Y maze (Moura et al. 2020), novel object recognition test (Moura et al. 2020), Barnes maze (Zappa Villar et al. 2018), and passive avoidance (Baluchnejadmojarad and Roghani 2006). Similarly, we observed such impairments in our ICV STZ group as shown by lower alternation in Y maze and decreased discrimination index in novel object recognition paradigm, higher number of errors and greater latency in the probe trial of Barnes maze, and reduction of step-through latency in passive avoidance test. In contrast, paeonol treatment of ICV STZ rats at the higher dose of 100 mg/kg properly attenuated all these cognitive dysfunctions. In line with our findings, it has shown that oral treatment with paeonol dose-dependently can improve isoflurane-induced cognitive dysfunction via regulating histone acetylation and JNK/ERK1/2/p38MAPK pathway (Jin et al. 2020), is capable to attenuate cognition deficits in STZ diabetic rat model of encephalopathy (Liu et al. 2013), and to ameliorate cognitive impairments induced by d-galactose in ICR mice (Zhong et al. 2009).

The brain tissue due to greater metabolic activity, high content of polyunsaturated fatty acids, and excessive oxygen consumption is vulnerable to free radicals (Nunomura et al. 2006; Wang et al. 2014). An imbalance between the generation of reactive oxygen species (ROS) and their removal by the enzymatic or non-enzymatic antioxidants causes the oxidative stress (Yang et al. 2020). In AD, part of cognitive decline is attributed to the development of oxidative stress associated with reduced antioxidants and concomitant mitochondrial impairment (Bivona et al. 2021). A similar condition also exists in ICV STZ model of AD (Salkovic-Petrisic et al. 2013). In the present study, following bilateral ICV injection of STZ, hippocampal oxidative stress was confirmed as shown by higher tissue level of MDA, ROS, and nitrite and lower quantities or activity of TAC, GSH, catalase, SOD, glutathione peroxidase (GPx), and glutathione reductase (GR). In contrast, paeonol treatment (100 mg/kg) of ICV STZ group mitigated oxidative stress burden, as demonstrated by reversal of most oxidative stress factors. In agreement with this finding, anti-oxidative effect of paeonol has been confirmed in STZ model of diabetes (Adki and Kulkarni 2021), in methyl-4-phenyl-1,2,3,6-tetrahydropyridine/probenecid model of Parkinson's disorder (Shi et al. 2016) and also in d-galactose (D-Gal)-induced model of cognitive dysfunction (Zhong et al. 2009). Excessive oxidative stress induces mitochondrial impairment with a derangement in ATP generation and altered calcium homeostasis and a further elevation of reactive oxygen species according to a positive feedback algorithm (Catanesi et al. 2020). STZ ICV in this study led to disturbed mitochondrial function, as evidenced by lower MMP that is in line with an earlier report (Wang et al. 2018). Conversely, paeonol administration was capable improve hippocampal MMP in ICV STZ group. Consistent with this finding, it has proved that paeonol can prevent excitotoxicity in PC12 cells via downregulation of ERK activation, inhibition of apoptosis, normalization of MMP, and cytochrome c release (Wang et al. 2011).

Moreover, oxidative stress following ICV injection of STZ is associated with a vicious cycle of neuroinflammatory events which further promotes oxidative stress (Cai et al. 2011; Maccioni et al. 2009). In the current study, ICV

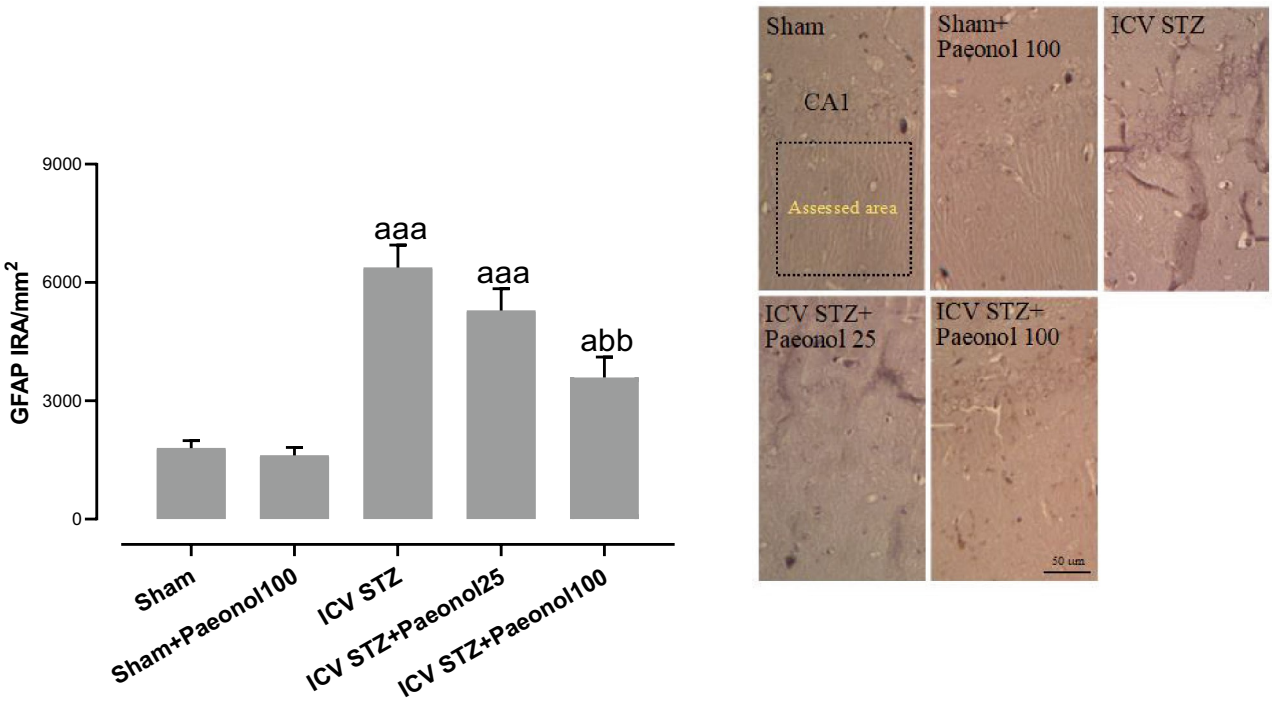

Fig. 4 Immunoreactivity for glial fibrillary acidic protein (GFAP) as a specific marker of astrocytes in hippocampal stratum radiatum and relevant photomicrographs. Results are brought as means ± SE. $n = 5$/group. [a] and [aaa] indicate $p < 0.05$ and $p < 0.001$, respectively (as compared to the sham group); [bb] indicate $p < 0.01$ (as compared to the ICV STZ group)

STZ group showed higher hippocampal level of TNFα and IL-6 in addition to prominent elevated immunoreactivity for GFAP as a specific marker of astrogliosis, all of which occur following neuroinflammation and as another prominent feature of AD pathogenesis (Fischer and Maier 2015; McGeer and McGeer 2003; Simpson and Oliver 2020). In contrast, paeonol administration at the higher dose successfully reduced hippocampal level of TNFa and IL-6 besides attenuating severity of astrogliosis. Consistent with these findings, it has shown that paeonol ameliorates CFA-induced inflammatory pain through partial suppression of HMGB1/TLR4/NF-κB signaling (Qiu et al. 2021), can inhibit methyl-4-phenyl-1,2,3,6-tetrahydropyridine/probenecid-induced model of Parkinson's disease (Shi et al. 2016), and is able to exert anti-neuroinflammatory effects in microglial cells which is partly mediated through inhibition of the production and release of nitric oxide (NO) and also suppression of the expression of inducible nitric oxide synthase (iNOS) and cyclooxygenase 2 (COX2) and also via reduction of ROS production and inhibition of ATP-induced cell migratory activity (Lin et al. 2015).

One of the most important neurotransmitters that play an essential role in both the peripheral and central nervous system is acetylcholine (ACh). In the brain of AD patients, acetylcholinesterase (AChE) activity in the brain undergoes a pathological increase. Our study showed that the paeonol significantly decreases the AChE activity as compared to the vehicle-treated ICV STZ group which may be responsible for part of improvement of cognitive impairments. Consistent with this finding, it has been shown that paeonol is a neuroprotective agent that can mitigate cognition deficits of diabetic encephalopathy in STZ model of diabetes in rats, partly through decreasing AChE activity in the hippocampal tissue (Liu et al. 2013). In addition to elevated activity of AChE, ICV STZ is also associated with enhanced activity of MPO as a reliable marker of neutrophil infiltration (Singh et al. 2013) that was also found out in this study. Paeonol at the higher dose of 100 mg/kg significantly attenuated hippocampal activity of MPO in the ICV STZ group. Consistent with finding regarding MPO, it has been shown that paeonol can dose-dependently reduce elevated MPO activity in carrageenan-injected paws in rats (Chou 2003).

To conclude, the current investigation demonstrated that paeonol can protect against cognitive dysfunctions in ICV STZ rat model of sAD which is somewhat mediated through mitigation of AChE, neuroinflammation, oxidative stress, mitochondrial dysfunction, and also via its diminution of astrogliosis.

Author Contribution Z.K. and M.R. designed the study, supervised conductance of experiments, and prepared the manuscript. M.R.

performed statistical analysis of data. A.TB. performed experiments and helped in manuscript writing.

Funding This research study was the results of PhD student thesis project that was approved by Faculty of Basic Sciences (Shahed University, Tehran, Iran) in 2020.

Availability of Data and Materials Data will be available on editor request.

Declarations

Ethics Approval and Consent to Participate All experimental procedures of this study were conducted under ethical committee supervision of Shahed University (Tehran, Iran) that was in accordance to NIH guidelines for the care and use of laboratory animals. All efforts were made to minimize number of animals and to lower their sufferings. Present study was approved by Institutional Ethics Committee of the Shahed University (Approval ID: IR.SHAHED.REC.1399.042).

Consent for Publication All authors have read the manuscript and approved its submission.

Competing Interests The authors declare no competing interests.

References

Adki KM, Kulkarni YA (2021) Neuroprotective effect of paeonol in streptozotocin-induced diabetes in rats. Life Sci 271:119–202

Ahshin-Majd S, Zamani S, Kiamari T, Kiasalari Z, Baluchnejadmojarad T, Roghani M (2016) Carnosine ameliorates cognitive deficits in streptozotocin-induced diabetic rats: Possible involved mechanisms. Peptides 86:102–111

Akhtar A, Dhaliwal J, Sah SP (2021) 7,8-Dihydroxyflavone improves cognitive functions in ICV-STZ rat model of sporadic Alzheimer's disease by reversing oxidative stress, mitochondrial dysfunction, and insulin resistance. Psychopharmacology (Berl)

Alzheimer's Association (2020) Alzheimer's disease facts and figures. Alzheimers Dement 16:391–460

Arya A, Sethy NK, Singh SK, Das M, Bhargava K (2013) Cerium oxide nanoparticles protect rodent lungs from hypobaric hypoxia-induced oxidative stress and inflammation. Int J Nanomedicine 8:4507–4520

Baluchnejadmojarad T, Roghani M (2006) Effect of naringenin on intracerebroventricular streptozotocin-induced cognitive deficits in rat: a behavioral analysis. Pharmacology 78(4):193–197

Benzie IF, Strain JJ (1996) The ferric reducing ability of plasma (FRAP) as a measure of antioxidant power: the FRAP assay. Anal Biochem 239(1):70–76

Bivona G, Lo Sasso B, Gambino CM, Giglio RV, Scazzone C, Agnello L, Ciaccio M (2021) The role of vitamin D as a biomarker in Alzheimer's disease. Brain Sci 11(3)

Cai Z, Zhao B, Ratka A (2011) Oxidative stress and β-amyloid protein in Alzheimer's disease. NeuroMol Med 13(4):223–250

Catanesi M, d'Angelo M, Tupone MG, Benedetti E, Giordano A, Castelli V, Cimini A (2020) MicroRNAs dysregulation and mitochondrial dysfunction in neurodegenerative diseases. Int J Mol Sci 21(17)

Chou TC (2003) Anti-inflammatory and analgesic effects of paeonol in carrageenan-evoked thermal hyperalgesia. Br J Pharmacol 139(6):1146–1152

Crous-Bou M, Minguillón C, Gramunt N, Molinuevo JL (2017) Alzheimer's disease prevention: from risk factors to early intervention. Alzheimers Res Ther 9(1):71

Ding J, Yu HL, Ma WW, Xi YD, Zhao X, Yuan LH, Feng JF, Xiao R (2013) Soy isoflavone attenuates brain mitochondrial oxidative stress induced by beta-amyloid peptides 1–42 injection in lateral cerebral ventricle. J Neurosci Res 91(4):562–567

Ellman GL, Courtney KD, Andres V Jr, Feather-Stone RM (1961) A new and rapid colorimetric determination of acetylcholinesterase activity. Biochem Pharmacol 7:88–95

Esterbauer H, Schaur RJ, Zollner H (1991) Chemistry and biochemistry of 4-hydroxynonenal, malonaldehyde and related aldehydes. Free Radical Biol Med 11(1):81–128

Fischer R, Maier O (2015) Interrelation of oxidative stress and inflammation in neurodegenerative disease: role of TNF. Oxid Med Cell Longev 2015:610813

Folch J, Petrov D, Ettcheto M, Abad S, Sánchez-López E, García ML, Olloquequi J, Beas-Zarate C, Auladell C, Camins A (2016) Current research therapeutic strategies for Alzheimer's disease treatment. Neural Plast 8501693

Guo Y, Du Y, Xie L, Pu Y, Yuan J, Wang Z, Zhang T, Wang B (2020) Effects of Paeonol and Gastroretention tablets of paeonol on experimental gastric ulcers and intestinal flora in rats. Inflammation 43(6):2178–2190

Han F, Xu H, Shen JX, Pan C, Yu ZH, Chen JJ, Zhu XL, Cai YF, Lu YP (2020) RhoA/Rock2/Limk1/cofilin1 pathway is involved in attenuation of neuronal dendritic spine loss by paeonol in the frontal cortex of D-galactose and aluminum-induced Alzheimer's disease-like rat model. Acta Neurobiol Exp (wars) 80(3):225–244

Jin H, Wang M, Wang J, Cao H, Niu W, Du L (2020) Paeonol attenuates isoflurane anesthesia-induced hippocampal neurotoxicity via modulation of JNK/ERK/P38MAPK pathway and regulates histone acetylation in neonatal rat. J Matern Fetal Neonatal Med 33(1):81–91

Khosravi Z, Sedaghat R, Baluchnejadmojarad T, Roghani M (2019) Diosgenin ameliorates testicular damage in streptozotocin-diabetic rats through attenuation of apoptosis, oxidative stress, and inflammation. Int Immunopharmacol 70:37–46

Kong D, Chen L, Huang W, Zhang Z, Wang L, Zhang F, Zheng S (2020) Combined therapy with ligustrazine and paeonol mitigates hepatic fibrosis through destroying mitochondrial integrity of stellate cell. Am J Transl Res 12(4):1255–1266

Kovacs GG (2017) Cellular reactions of the central nervous system. Handb Clin Neurol 145:13–23

Lin C, Lin HY, Chen JH, Tseng WP, Ko PY, Liu YS, Yeh WL, Lu DY (2015) Effects of paeonol on anti-neuroinflammatory responses in microglial cells. Int J Mol Sci 16(4):8844–8860

Liu J, Feng L, Ma D, Zhang M, Gu J, Wang S, Fu Q, Song Y, Lan Z, Qu R, Ma S (2013) Neuroprotective effect of paeonol on cognition deficits of diabetic encephalopathy in streptozotocin-induced diabetic rat. Neuroscience letters 549:63–68

Ma W, Yuan L, Yu H, Ding B, Xi Y, Feng J, Xiao R (2010) Genistein as a neuroprotective antioxidant attenuates redox imbalance induced by beta-amyloid peptides 25–35 in PC12 cells. Int J Dev Neurosci 28(4):289–295

Maccioni RB, Rojo LE, Fernández JA, Kuljis RO (2009) The role of neuroimmunomodulation in Alzheimer's disease. Ann NY Acad Sci 1153:240–246

Martins M, Silva R, MM Pinto M, Sousa E (2020) Marine natural products, multitarget therapy and repurposed agents in Alzheimer's disease. Pharmaceuticals (Basel) 13(9)

Masters CL, Bateman R, Blennow K, Rowe CC, Sperling RA, Cummings JL (2015) Alzheimer's disease. Nat Rev Dis Primers 1:15056

McGeer EG, McGeer PL (2003) Inflammatory processes in Alzheimer's disease. Prog Neuropsychopharmacol Biol Psychiatry 27(5):741–749

Mohamad Nasir NF, Zainuddin A, Shamsuddin S (2018) Emerging roles of Sirtuin 6 in Alzheimer's disease. J Mol Neurosci 64(2):157–161

Mohandas J, Marshall JJ, Duggin GG, Horvath JS, Tiller DJ (1984) Differential distribution of glutathione and glutathione-related enzymes in rabbit kidney. Possible implications in analgesic nephropathy. Biochem Pharmacol 33(11):1801–1807

Moura ELR, Dos Santos H, Celes APM, Bassani TB, Souza LC, Vital M (2020) Effects of a nutritional formulation containing caprylic and capric acid, phosphatidylserine, and docosahexaenoic acid in Streptozotocin-lesioned rats. J Alzheimers Dis Rep 4(1):353–363

Nasri S, Roghani M, Baluchnejadmojarad T, Balvardi M, Rabani T (2012) Chronic cyanidin-3-glucoside administration improves short-term spatial recognition memory but not passive avoidance learning and memory in streptozotocin-diabetic rats. Phytother Res 26(8):1205–1210

Nunomura A, Castellani RJ, Zhu X, Moreira PI, Perry G, Smith MA (2006) Involvement of oxidative stress in Alzheimer disease. J Neuropathol Exp Neurol 65(7):631–641

Oba H, Kadoya Y, Okamoto H, Matsuoka T, Abe Y, Shibata K, Narumoto J (2021) The economic burden of dementia: evidence from a survey of households of people with dementia and their caregivers. Int J Environ Res Public Health 18(5)

Ojha S, Javed H, Azimullah S, Abul Khair SB, Haque ME (2015) Neuroprotective potential of ferulic acid in the rotenone model of Parkinson's disease. Drug Des Devel Ther 9:5499–5510

Olszewska-Słonina DM, Mątewski D, Czajkowski R, Olszewski KJ, Woźniak A, Odrowąż-Sypniewska G, Lis K, Musiałkiewicz D, Kowaliszyn B (2011) The concentration of thiobarbituric acid reactive substances (TBARS) and paraoxonase activity in blood of patients with osteoarthrosis after endoprosthesis implantation. Med Sci Monit 17(9):CR498–CR504

Pulli B, Ali M, Forghani R, Schob S, Hsieh KL, Wojtkiewicz G, Linnoila JJ, Chen JW (2013) Measuring myeloperoxidase activity in biological samples. PLoS One 8(7):e67976

Qiu C, Yang LD, Yu W, Tian DD, Gao MR, Wang WJ, Li XB, Wu YM, Wang M (2021) Paeonol ameliorates CFA-induced inflammatory pain by inhibiting HMGB1/TLR4/NF-κB p65 pathway. Metab Brain Dis 36(2):273–283

Ramazi S, Fahanik-Babaei J, Mohamadi-Zarch SM, Tashakori-Miyanroudi M, Nourabadi D, Nazari-Serenjeh M, Roghani M, Baluchnejadmojarad T (2020) Neuroprotective and anticonvulsant effects of sinomenine in kainate rat model of temporal lobe epilepsy: Involvement of oxidative stress, inflammation and pyroptosis. J Chem Neuroanat 108:101800

Rani R, Kumar A, Jaggi AS, Singh N (2021) Pharmacological investigations on efficacy of Phlorizin a sodium-glucose co-transporter (SGLT) inhibitor in mouse model of intracerebroventricular streptozotocin induced dementia of AD type. J Basic Clin Physiol Pharmacol

Salkovic-Petrisic M, Knezovic A, Hoyer S, Riederer P (2013) What have we learned from the streptozotocin-induced animal model of sporadic Alzheimer's disease, about the therapeutic strategies in Alzheimer's research. J Neural Transm (Vienna, Austria: 1996) 120(1):233–252

Sharma Y, Garabadu D (2020) Ruthenium red, mitochondrial calcium uniporter inhibitor, attenuates cognitive deficits in STZ-ICV challenged experimental animals. Brain Res Bull 164(121–135

Shi X, Chen YH, Liu H, Qu HD (2016) Therapeutic effects of paeonol on methyl-4-phenyl-1,2,3,6-tetrahydropyridine/probenecid-induced Parkinson's disease in mice. Mol Med Rep 14(3):2397–2404

Simpson DSA, Oliver PL (2020) ROS generation in microglia: understanding oxidative stress and inflammation in neurodegenerative disease. Antioxidants (Basel, Switzerland) 9(8)

Singh B, Sharma B, Jaggi AS, Singh N (2013) Attenuating effect of lisinopril and telmisartan in intracerebroventricular streptozotocin induced experimental dementia of Alzheimer's disease type: possible involvement of PPAR-γ agonistic property. J Renin Angiotensin Aldosterone Syst 14(2):124–136

Stuart SA, Robertson JD, Marrion NV, Robinson ES (2013) Chronic pravastatin but not atorvastatin treatment impairs cognitive function in two rodent models of learning and memory. PLoS One 8(9):e75467

Uddin MS, Mamun AA, Hossain MS, Akter F, Iqbal MA, Asaduzzaman M (2016) Exploring the effect of Phyllanthus emblica L. on cognitive performance, brain antioxidant markers and acetylcholinesterase activity in rats: promising natural gift for the mitigation of Alzheimer's disease. Ann Neurosci 23(4):218–229

Verma V, Singh D, Kh R (2020) Sinapic acid alleviates oxidative stress and neuro-inflammatory changes in sporadic model of Alzheimer's disease in Rats. Brain Sci 10(12)

Walker JM (1996) The Bicinchoninic Acid (BCA) Assay for protein quantitation. In: Walker JM (ed) The protein protocols handbook. Humana Press, Totowa, NJ, pp 11–14

Wang D, Liu L, Li S, Wang C (2018) Effects of paeoniflorin on neurobehavior, oxidative stress, brain insulin signaling, and synaptic alterations in intracerebroventricular streptozotocin-induced cognitive impairment in mice. Physiol Behav 191:12–20

Wang X, Wang W, Li L, Perry G, Lee HG, Zhu X (2014) Oxidative stress and mitochondrial dysfunction in Alzheimer's disease. Biochem Biophys Acta 1842(8)1240–1247

Wang X, Zhu G, Yang S, Wang X, Cheng H, Wang F, Li X, Li Q (2011) Paeonol prevents excitotoxicity in rat pheochromocytoma PC12 cells via downregulation of ERK activation and inhibition of apoptosis. Planta Med 77(15):1695–1701

Wopara I, Modo EU, Adebayo OG, Mobisson SK, Nwigwe JO, Ogbu PI, Nwankwo VU, Ejeawa CU (2021) Anxiogenic and memory impairment effect of food color exposure: upregulation of oxido-neuroinflammatory markers and acetyl-cholinestrase activity in the prefrontal cortex and hippocampus. Heliyon 7(3):e06378–e06378

Yang N, Guan QW, Chen FH, Xia QX, Yin XX, Zhou HH, Mao XY (2020) Antioxidants targeting mitochondrial oxidative stress: promising neuroprotectants for epilepsy. Oxid Med Cell Longev 6687185

Ye M, Yi Y, Wu S, Zhou Y, Zhao D (2017) Role of paeonol in an astrocyte model of Parkinson's disease. Medical science monitor: international medical journal of experimental and clinical research 23:4740–4748

Zameer S, Kaundal M, Vohora D, Ali J, Kalam Najmi A, Akhtar M (2019) Ameliorative effect of alendronate against intracerebroventricular streptozotocin induced alteration in neurobehavioral, neuroinflammation and biochemical parameters with emphasis on Aβ and BACE-1. Neurotoxicology 70:122–134

Zappa Villar MF, López Hanotte J, Falomir Lockhart E, Trípodi LS, Morel GR, Reggiani PC (2018) Intracerebroventricular streptozotocin induces impaired Barnes maze spatial memory and reduces astrocyte branching in the CA1 and CA3 hippocampal regions. J Neural Transm (vienna) 125(12):1787–1803

Zappa Villar MF, López Hanotte J, Pardo J, Morel GR, Mazzolini G, García MG, Reggiani PC (2020) Mesenchymal stem cells therapy improved the Streptozotocin-induced behavioral and Hippocampal impairment in rats. Mol Neurobiol 57(2):600–615

Zhao B, Shi QJ, Zhang ZZ, Wang SY, Wang X, Wang H (2018) Protective effects of paeonol on subacute/chronic brain injury during cerebral ischemia in rats. Exp Ther Med 15(4):3836–3846

Zhong SZ, Ge QH, Qu R, Li Q, Ma SP (2009) Paeonol attenuates neurotoxicity and ameliorates cognitive impairment induced by d-galactose in ICR mice. J Neurol Sci 277(1–2):58–64

Zhu Y, Peng L, Hu J, Chen Y, Chen F (2019) Current anti-Alzheimer's disease effect of natural products and their principal targets. J Integr Neurosci 18(3):327–339